Evaluation of the influence of the main plasma density parameters on antenna coupling and radio frequency potentials with TOPICA code

2013 Plasma Phys. Control. Fusion 55 045010

(http://iopscience.iop.org/0741-3335/55/4/045010)

Plasma Phys. Control. Fusion **55** (2013) 045010 (9pp) doi:10.1088/0741-3335/55/4/045010

Evaluation of the influence of the main plasma density parameters on antenna coupling and radio frequency potentials with TOPICA code

D Milanesio[1] **and R Maggiora**

Politecnico di Torino, Dipartimento di Elettronica e Telecomunicazioni (DET), Torino, Italy

E-mail: daniele.milanesio@polito.it

Received 13 November 2012, in final form 18 February 2013
Published 13 March 2013
Online at stacks.iop.org/PPCF/55/045010

Abstract
The successful design of an ion cyclotron antenna mainly relies on the capability of accurately predicting its behavior both in terms of input parameters, and therefore power coupled to plasma, and radiated fields. All these features essentially depend on the antenna itself (its geometry, the matching and tuning systems) and, obviously, on the faced loading. In this paper a number of plasma profiles is analysed with the help of the TOPICA code, a predictive tool for the design and optimization of radio frequency (RF) launchers in front of a plasma, in order to understand which plasma parameters have the most significant influence on the coupling performances of a typical IC antenna.

(Some figures may appear in colour only in the online journal)

1. Motivation and background

Ion cyclotron (IC) antennas are a key part of most of the present-day experiments toward the realization of controlled nuclear fusion with magnetic confinement, and will certainly play a fundamental role also for the next generation of tokamaks such as ITER or DEMO.

That being so, it is of paramount importance to have a reliable numerical tool that can assist their design, providing accurate predictions in terms of input parameters, transferred power and radiated fields. In particular, this last topic is extremely important in view of those unwanted phenomena, such as rectification discharges or hot spots, that are naturally associated with the required power levels and that can completely prevent an IC antenna from correctly working.

These needs motivated, almost a decade ago, the development of the TOPICA code [1], which was the only code able to account both for realistic 3D geometries and for an accurate 1D plasma model. Several upgrades have been introduced in recent years in order to reduce the distance between TOPICA simulations and real life experiments. To provide few examples, the multi-cavity formulation [2] and the full code parallelization, together with the huge computing power nowadays available, allowed us to remove all limitations in terms of geometrical precision, as documented in [3–5]; in all the aforementioned works, the IC launchers were directly imported from CAD drawings without introducing any significant simplification. Furthermore, the importance of the geometrical accuracy was also pointed out in [6], where the performances of a realistic curved launcher were compared with the ones obtained by its flat version (both 3D).

The aim of this paper is instead to investigate the influence of the plasma profile in the TOPICA code, presenting a detailed analysis similar to [7]. A preliminary study of this sort was already depicted in [6, 8]; we would like to extend here that exercise and provide a more complete picture of the problem. In proposing this study, we are fully aware that the presented results will be intrinsically connected to the plasma model coupled to TOPICA, i.e. to the 1D FELICE code [9]. However, while working to upgrade TOPICA to a more realistic plasma code, such as the fully 3D TORIC code [10], we would like to stress in this work which are the most important parameters playing a role and, to some extent, which are the limits of our current model.

This paper is divided as follows: an overview of the adopted geometry and of the simulated plasma profiles is given

[1] Author to whom any correspondence should be addressed.

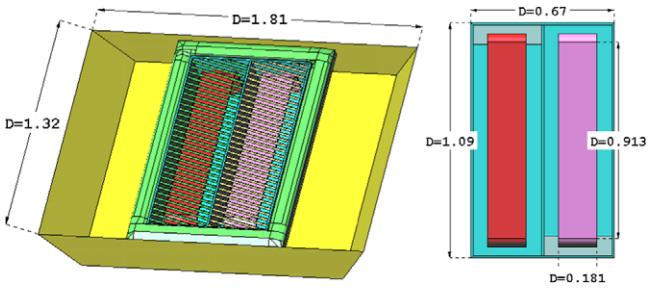

Figure 1. Front views of the 3D flat IC launcher simulated with TOPICA with some relevant dimensions (in m).

in section 2, while section 3 contains the results of the analysis with the TOPICA code.

2. Description of TOPICA setup

2.1. The simulation tool

As already anticipated, all the results outlined in this work were produced with the help of the TOPICA code. While referring the interested reader to [1, 2] for a more detailed analysis of the code formulation, we would like to shortly describe here the features that were specifically exploited in this paper. In particular, together with the evaluation of the antenna input parameters and, therefore, of the power transferred to plasma, the code also allows us to calculate the electric field map everywhere inside the antenna enclosure and the plasma region. In addition, by means of a specific post-processing tool that computes the integral of the parallel component of the electric field along the magnetic field lines in a realistic 3D geometry, the user can determine the parallel radio frequency (RF) potentials in front of the launcher. To conclude the overview, the FELICE code [9] takes into account the interaction with plasma, affording 1D density and temperature profiles, and finite Larmor radius (FLR) effects. In short, FELICE performs a k_y, k_z Fourier analysis and a numerical integration in the space domain along the radial direction.

2.2. The IC launcher

Since the focus of this paper is to exploit the sensitivity of the results (delivered power and RF potentials) to the variation of the main plasma parameters, we opted for a 3D flat launcher, as reported in figures 1 and 2. The adopted geometry shares most of the typical features of the existing IC antenna: it has two straights currents straps which are independently fed by 25 Ω lines (located on the left side of the antenna and connected to the straps by means of a piece of matched stripline hidden in the back), a vertical central septum that separates the two radiating elements, limiter tiles positioned all around the antenna box and a tilted Faraday screen (11°). The general dimensions of the adopted model are comparable to the flat geometry corresponding to one of the ASDEX-Upgrade IC antennas (see figure 3 in [8] or figure 1 in [6]): as a matter of fact, the 3D curved version of this launcher could perfectly fit into one of the ASDEX-Upgrade IC ports. Also the operating

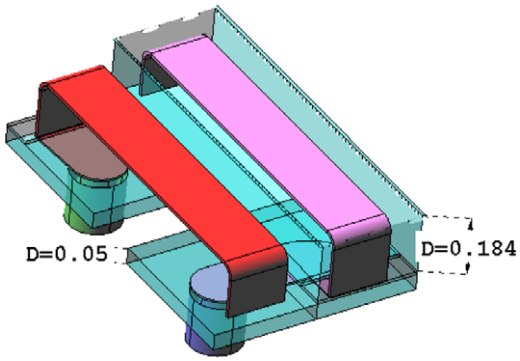

Figure 2. Zoomed front view, with dimensions (in m), of the two straight straps and their stripline connection to the coaxial cables. A 5 cm wide metallic box is designed to completely separate the feeding stripline from the front part of the antenna structure housing the current straps.

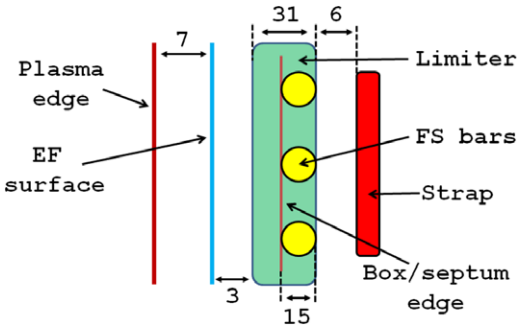

Figure 3. Simplified sketch (not in scale) of a side view of the launcher, with dimensions (in mm); the radial position of the main antenna elements is reported, together with the location of the plasma edge.

frequency, namely 30 MHz, is coherent with the ASDEX-Upgrade experiment.

To better underline the radial position of the main elements of the antenna (straps, FS bars, limiter) and of the plasma edge, figure 3 reports a schematic side view of the launcher. As detailed in section 3, the electric field distribution was computed in two different locations, i.e. at the plasma interface and on an electric field plane (EF surface in the picture) closer to the limiters; in both cases, the integration domain corresponds to the size of the antenna cavity (in yellow, on the left of figure 1).

2.3. The simulated plasma profiles

A reference density profile has been tailored according to measured plasma profiles from ASDEX-Upgrade experimental activity (major radius equal to 1.65 m). As one can notice from figure 4, the reference density curve is within the range of the measured profiles; moreover, four distinct areas are underlined in the picture (plateau, inner gradient, outer gradient, edge) and will be used in the following sections to better describe the performed tests. Generally speaking, this is a typical minority heating scenario, with 97% deuterium and 3% hydrogen, with central temperature around 1.45 keV and central static magnetic field of 2 T. With a 0π input phasing (imposed on the strap front surface), the power spectrum has a maximum

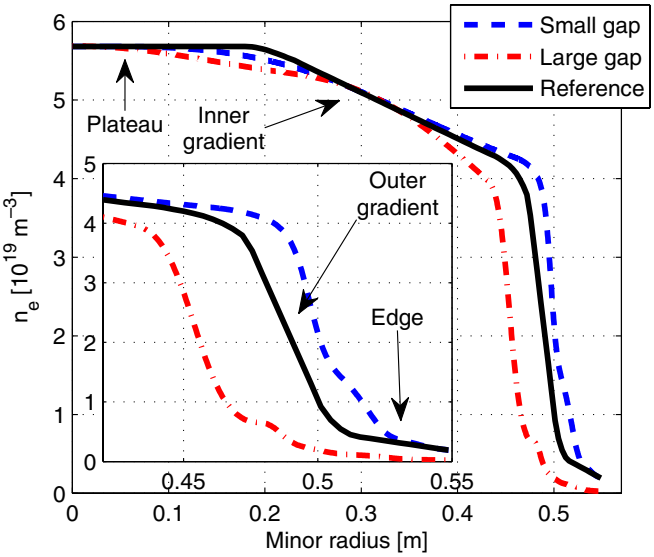

Figure 4. Measured density profiles ('small gap' in dashed blue, 'large gap' in dashed-dotted red) compared with the density profile (black solid curve) adopted as a reference for TOPICA tests. The reference profile is divided into four sections which are labeled, starting from the center of the plasma region, as plateau, inner gradient, outer gradient and edge.

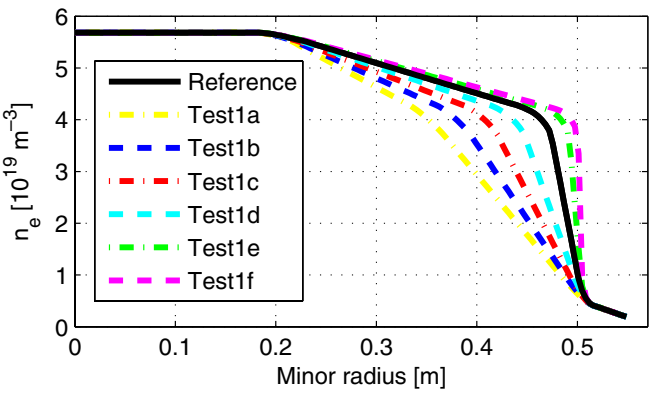

Figure 5. Test1(a–f) profiles (dashed lines, from left to right) obtained from the reference curve (solid black line) varying the two density gradients.

around $k_\parallel = 12\,\mathrm{m}^{-1}$, corresponding to a cut-off density of about $1.1 \times 10^{19}\,\mathrm{m}^{-3}$ (located approximately 5 cm from the plasma edge).

It is worth mentioning that the so-called TOPICA *aperture* (see [1] for further details), which corresponds to the interface between the antenna region (in vacuum) and the plasma region, is located where the density curve stops, i.e. at 0.5487 m from the center of the torus section.

Adopting our reference scenario as a starting point, we first varied the two density gradients (inner and outer gradient), keeping constant both the central density (plateau) and the final part of the profile (edge); figure 5 shows the complete set of Test1 simulated profiles.

We then modified only the last 4 cm of the profile (edge), varying the edge density from a minimum of about $9.5 \times 10^{16}\,\mathrm{m}^{-3}$ (Test2a) to a maximum of about $0.4 \times 10^{19}\,\mathrm{m}^{-3}$ (Test2d); all the Test2 simulated profiles are reported in figure 6.

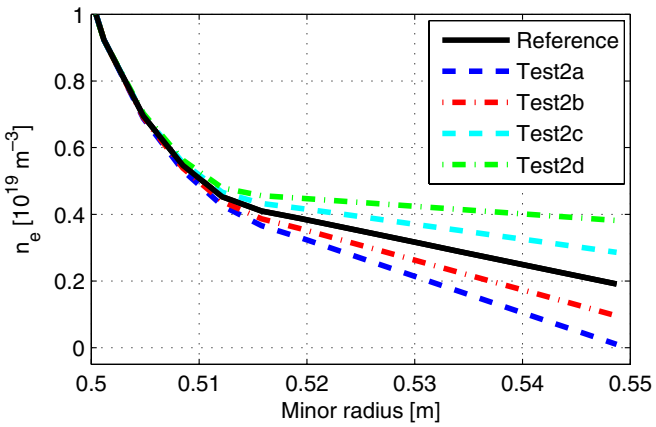

Figure 6. Test2(a–d) profiles (dashed lines, from bottom to top) obtained from the reference curve (solid black line) varying the edge density.

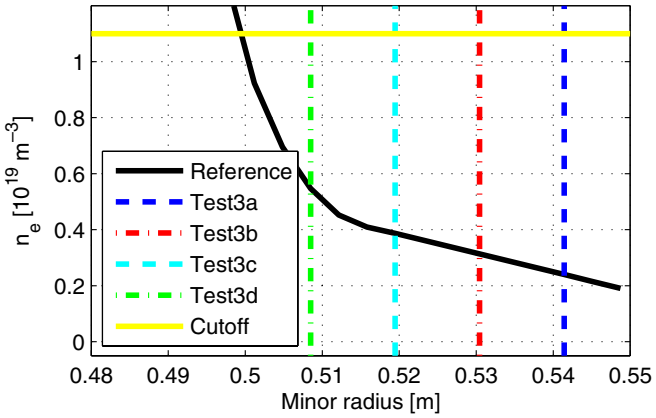

Figure 7. Test3(a–f) profiles (dashed lines, from right to left) obtained from the reference curve (solid black line). The loaded profile stops at the radial position indicated by the dashed line, the missing portion is substituted by an equivalent (in length) vacuum layer. The plain horizontal line indicates the cut-off density for the dominant mode.

The third group of simulated density profiles was tailored to exploit the dependence on the *equivalent* vacuum layer: starting from the reference profile, we progressively substituted a portion of the edge (low) density plasma with a vacuum layer of identical length, i.e. keeping constant the distance between the antenna and the fast wave cut-off position. The equivalent vacuum goes from a minimum of 7.3 mm (Test3a) to a maximum of 40.2 mm (Test3d). Figure 7 reports the radial position where each plasma profile was truncated.

In the fourth and fifth set of profiles we varied the central density, adopting two slightly different approaches. In one case (Test4) we changed the length of the inner gradient section and of the plateau (keeping constant their sum), reducing or increasing the size of the first in favor of the second; in the other group of tests (Test5) we only vertically shifted both the inner gradient curve and the plateau, without changing their size. Figure 8 and 9 document the differences among the loaded density profiles.

The last test dealt with the plasma temperature; starting from the reference temperature profile, we increased it up to

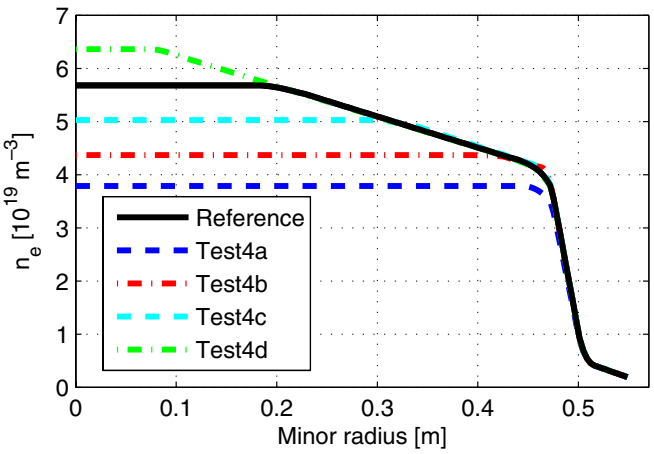

Figure 8. Test4(a–d) profiles (dashed lines, from bottom to top) obtained from the reference curve (solid black line) varying the central density.

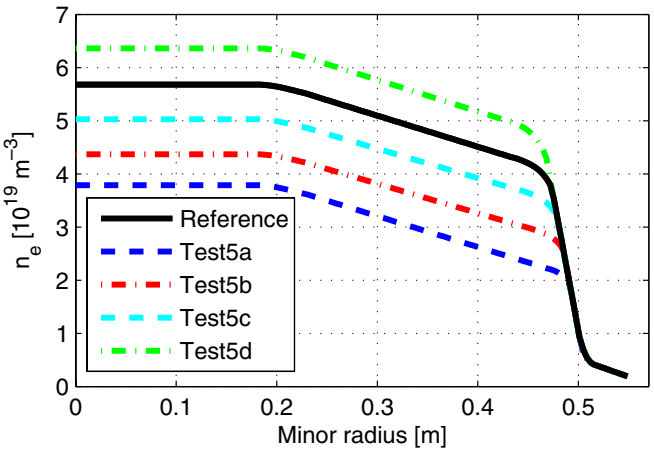

Figure 9. Test5(a–d) profiles (dashed lines, from bottom to top) obtained from the reference curve (solid black line) varying the central density.

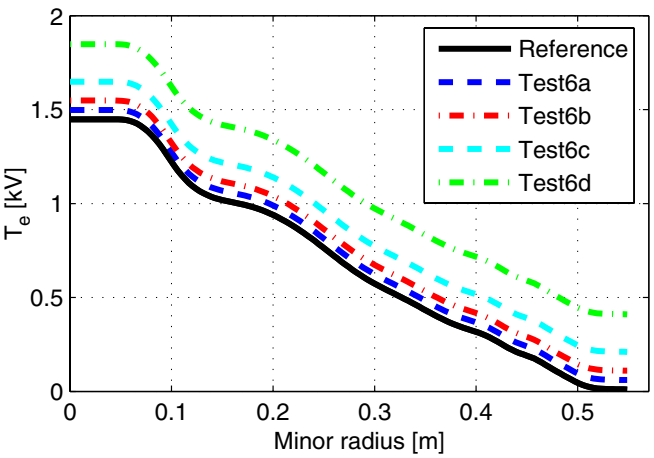

Figure 10. Test6(a–d) profiles (dashed lines, from bottom to top) obtained from the reference curve (solid black line) varying the whole temperature (ion and electron) profile.

a central value of 1.84 keV (+30%), as reported in figure 10. It is important to mention that the same temperature profile is adopted for both ions and electrons.

3. Results

In this section, we present the effects of the loaded plasma profiles on the antenna input parameters and electric fields. To be more specific, we computed the power transferred to plasma (which directly depends on the impedance matrix of the launcher) in the absence of a tuning and matching system, i.e. considering coaxial cables of infinite length connected to each input port of the antenna and a maximum voltage along these cables equal to 30 kV. Then, moving to the RF potentials, we evaluated the electric field maps at two radial positions in front of the antenna, i.e. at 3 mm from the limiters (inside the antenna region, in vacuum) and at 10 mm from the limiters (at the interface with the plasma edge). Moreover, we calculated, on both surfaces, the integral of the parallel electric field (shown in magnitude in the next pictures) and the integral of its absolute value along the magnetic field lines, normalized to 1 MW of coupled power. Please note that the magnetic field is always assumed to be perfectly aligned with the the Faraday screen rods, which are tilted of 11° with respect to the toroidal axis.

3.1. FELICE tuning

While most of the input parameters of FELICE are directly linked to the loaded density and temperature plasma profiles (and are therefore univocally set), some of them are instead related to the numerical solution of the implemented differential equations and, as a consequence, need to be tuned in order to reach convergence. In particular, we would like to spend few words here on the position of the outward radiating condition, i.e. where the launched waves are considered to be fully absorbed, and on the spatial resolution, i.e. on the radial sampling adopted to discretize the loaded curves.

For our reference profile, the waves (in particular the fast wave) appear to radiate only in the outward direction after approximately 10 cm from the plasma edge and 5 cm from the fast wave cut-off (single pass absorption). Practically speaking, this means that the user can neglect the remaining part of the profile, whose shape will not influence the output of FELICE; otherwise said, imposing the wave outward radiation condition after more than 10 cm has the only consequence of increasing the computation time, but no impact at all on the estimated antenna performances. Conversely, imposing the outward radiation condition before 10 cm would determine a significant inaccuracy in the plasma response. Unfortunately the position of this point may be shifted of several centimeters with a different density profile; that being so, we set this value to 30 cm for all the following tests.

Coming to the second parameter, we verified that a spatial resolution of the order of few millimeters is enough to reach stable results with the reference profile. However, this has to be increased to correctly sample density profiles characterized by very steep gradients: once more, we opted for a slightly time consuming over sampling with a resolution of fractions of millimeters to be sure of getting convergence for all the simulated cases.

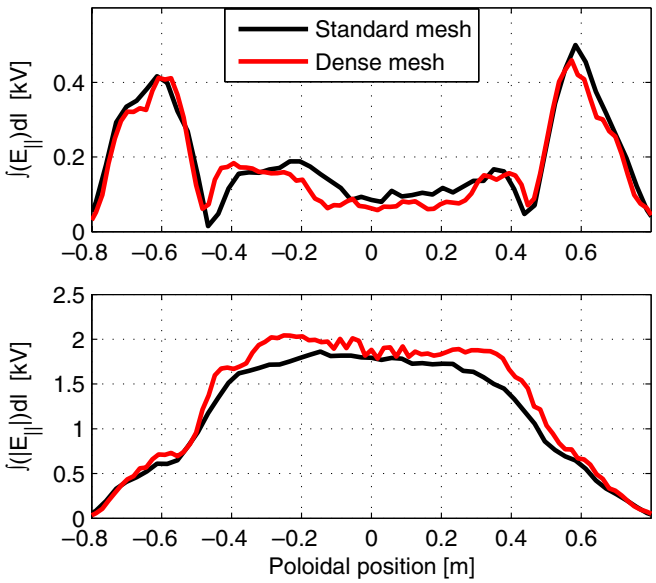

Figure 11. RF potentials (in kV) computed at the plasma interface (10 mm from the antenna limiters), integrating the parallel electric field (top, in magnitude) and its absolute value (bottom) along the magnetic field lines.

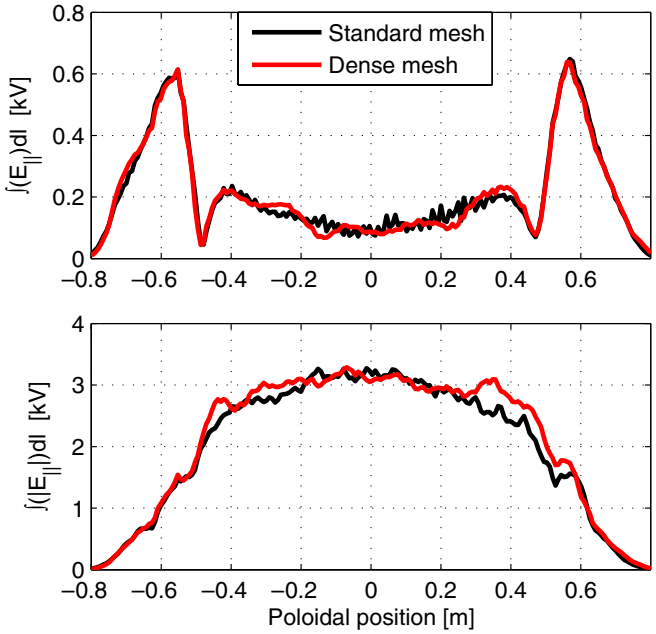

Figure 12. RF potentials (in kV) computed in front of the limiters (3 mm), integrating the parallel electric field (top, in magnitude) and its absolute value (bottom) along the magnetic field lines.

3.2. Mesh influence

Before starting with the evaluation of the plasma effects, we report a short analysis of the mesh influence. As any other numerical tool, also TOPICA results depend on the quality of the adopted mesh, i.e. on the density of the triangular elements that are used to discretize the launcher (see [1] for more details about the chosen functions); on the one side, one would like to use enough elements to reach convergence, on the other side to avoid over sampling, which practically means wasted cpu time. Our past experience underlined that code results are influenced above all by the resolution adopted at the interface between the antenna region and the plasma one, while the mesh on the launcher itself, provided it is reasonably dense, is not that important. As one may guess, an accurate description of the interface with plasma is of crucial importance if one wants to correctly account for the interaction with it.

Starting with a standard mesh density characterized by 2700 unknowns at the plasma interface, corresponding to a spatial resolution of about 7 cm, we increased the mesh up to a maximum of 7200 unknowns, corresponding to a 4.5 cm resolution. In terms of cpu time, the increase in functions doubled the computation time (from 1 h to 2 h with 576 cores) when running the plasma module of the code. Coming to the results, the calculated coupled power remained constant for all tests, proving that the input parameters already converged to their final value with the standard mesh. Conversely, a small difference was observed for the RF potentials, as the reader can notice in figure 11.

While the electric field varied a bit on the aperture (10 mm from the limiters), figure 12 reports a substantial stability of the results computed on the electric field surface (3 mm in front of the limiters, in vacuum), where the mesh resolution was kept constant to 9 mm for all tests. In this case one may note that few millimeters of distance between those two surfaces are enough to smooth the results and remove any mesh dependence.

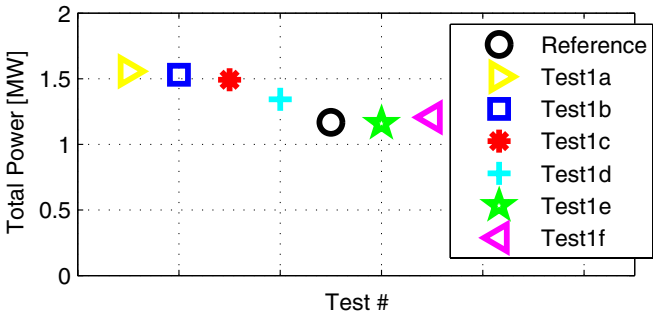

Figure 13. Power transferred to plasma (in MW) versus density gradient, assuming infinite coaxial lines connected to the ports, with a maximum voltage of 30 kV along the lines.

Given the small variation of the code outputs, we kept the standard mesh geometry as our reference choice for the remaining tests. Furthermore, the RF potentials will be always shown on the electric field surface located 3 mm in front of the limiters; the higher resolution of the mesh imposed to that surface guarantees more accurate and stable results.

3.3. Test1: density gradient

The variation of the density gradient has a considerable influence on the power transferred to plasma, as figure 13 clearly demonstrates: profiles characterized by smoother gradients allow a far better coupling (+25%) than steep density gradients. However, the reader can also notice that there seems to be a sort of asymptotic convergence of the results: when the gradient is very smooth (but also when it becomes very steep),

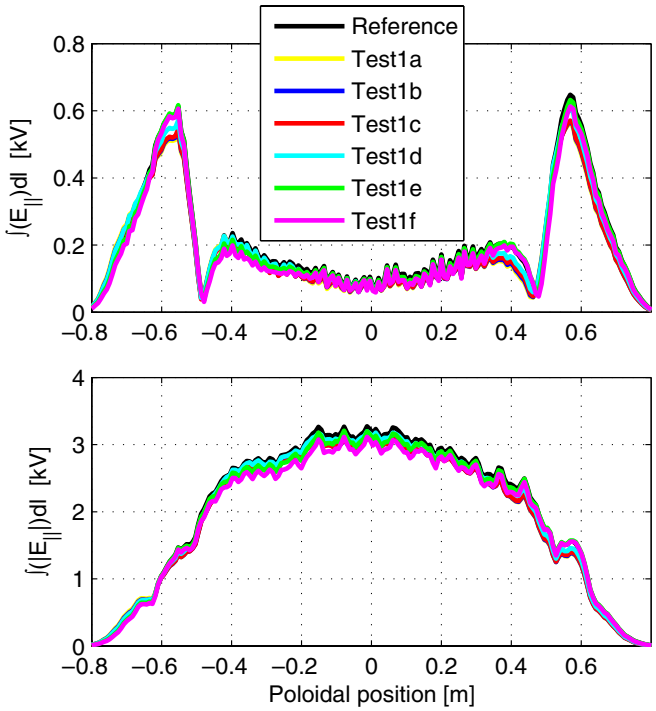

Figure 14. RF potentials (in kV) versus density gradient, computed integrating the parallel electric field (top, in magnitude) and its absolute value (bottom) along the magnetic field lines.

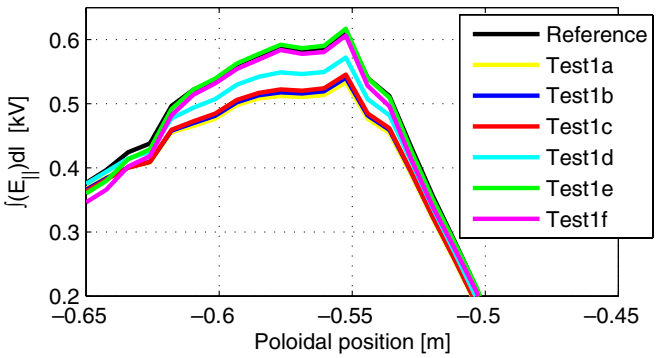

Figure 15. Zoomed view of the top graph in figure 14: the left peak, corresponding to the RF potentials computed along lines crossing the bottom part of the antenna, is shown.

a further decrease (or increase) in the slope of the curve does not significantly change the performances of the antenna.

Moving to the analysis of the electric fields, figure 14 shows the corresponding RF potentials: we can definitely affirm that the variation of the density gradient does not considerably affect the RF potentials. Despite this, looking at the zoomed view of one of the peaks (figure 15), one may also see that the maximum value is found in correspondence to the steeper gradients and, in general, the peak magnitude decreases with the decrease in the gradient. As for the power to plasma, the same asymptotic behavior is observed here: the differences between the reference profile and Test1e or Test1f cases are practically negligible (black, green and magenta curves are almost overlapped), while a small gap is found between the reference profile and Test1d case.

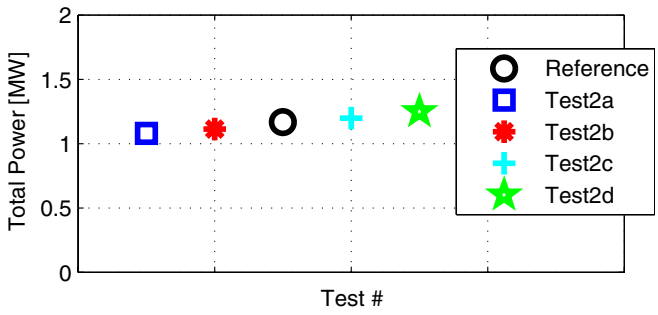

Figure 16. Power transferred to plasma (in MW) versus edge density, assuming infinite coaxial lines connected to the ports, with a maximum voltage of 30 kV along the lines.

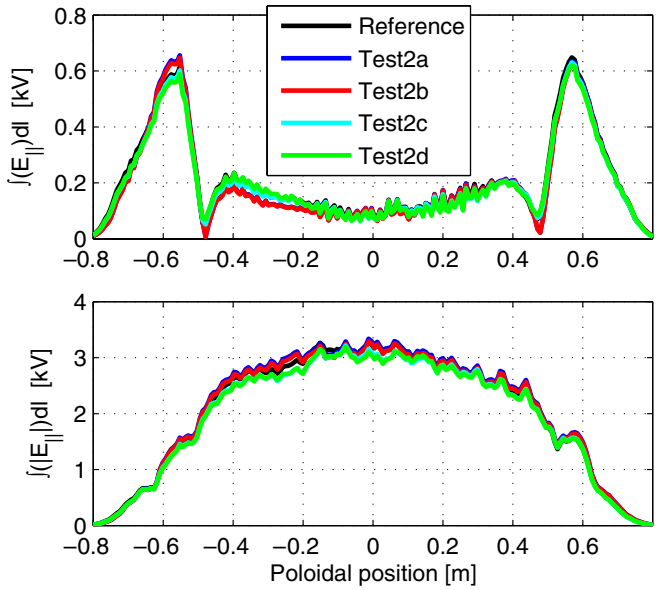

Figure 17. RF potentials (in kV) versus edge density, computed integrating the parallel electric field (top, in magnitude) and its absolute value (bottom) along the magnetic field lines.

3.4. Test2: edge density

Figure 16 reports stronger power to plasma for the profiles with higher edge density. It must be stressed that, for this second group of tests, the difference among the simulated cases is rather small (within 10%); this is mainly due to the fact that we varied a portion of the density profile which is below the cut-off for the dominant mode.

Concerning the RF potentials, figure 17 shows no considerable variation depending on the edge density. The zoomed view reported in figure 18 allows instead to notice that the peak magnitude slightly decreases with the increase in the edge density.

3.5. Test3: equivalent vacuum

As alluded in section 2.3, one would expect that the replacement of a portion of low density plasma (clearly below the fast wave cut-off for the dominant mode) with an equivalent (in length) layer of vacuum should not modify the performances of the antenna, at least in terms of power

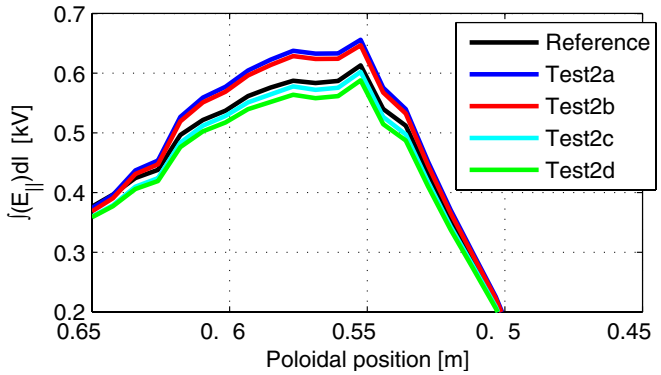

Figure 18. Zoomed view of the top graph in figure 17: the left peak, corresponding to the RF potentials computed along lines crossing the bottom part of the antenna, is shown.

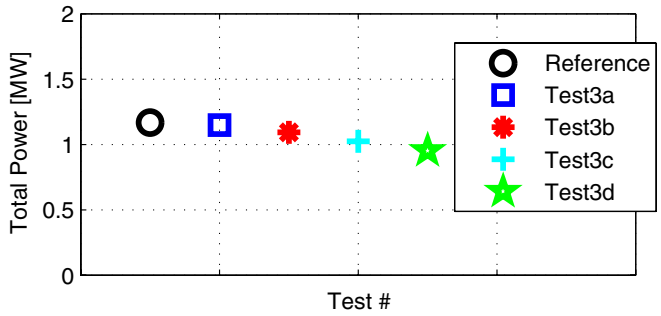

Figure 19. Power transferred to plasma (in MW) versus equivalent vacuum, assuming infinite coaxial lines connected to the ports, with a maximum voltage of 30 kV along the lines.

coupled to plasma; as a matter of fact, figure 19 demonstrates that the power variation is rather small, namely within 10%. However, the reader should also notice that there definitely is a decrease in the transferred power when the low density plasma is replaced with vacuum, which can be mainly attributed to the higher mismatch caused by the increasing difference (in density) between the vacuum gap and the edge density value.

Rather different conclusions have to be drawn when analyzing the RF potentials: the equivalent vacuum plays a fundamental role in this case, as reported in figure 20, determining a 50% increase in the potentials on some areas in front of the antenna.

In general, we can affirm that, if the user is interested in investigating the coupling performances of an IC launcher, the very first centimeters of the plasma density profile are not so relevant; practically speaking, this is also the region where the measurements are usually affected by the largest errors. Provided that the profile is accurately known after (and around) the fast wave cut-off position, in the case of uncertainties one can also replace a part of the profile with an equivalent vacuum layer without considerably affecting the power transferred to plasma. Conversely, if the user is interested in knowing, with a great precision, the electric field distribution in front of the antenna, the aforementioned procedure (the use of equivalent vacuum) has to be avoided.

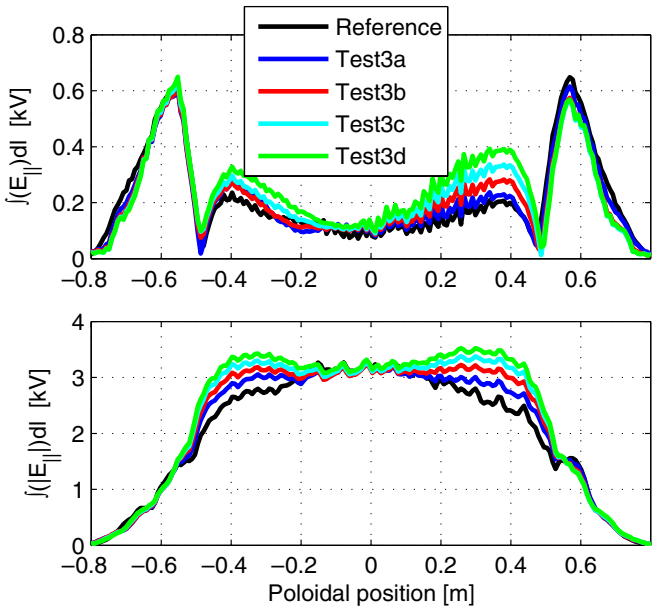

Figure 20. RF potentials (in kV) versus equivalent vacuum, computed integrating the parallel electric field (top, in magnitude) and its absolute value (bottom) along the magnetic field lines.

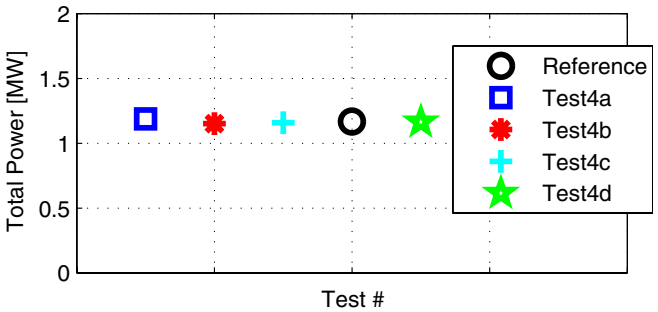

Figure 21. Power transferred to plasma (in MW) versus central density, assuming infinite coaxial lines connected to the ports, with a maximum voltage of 30 kV along the lines.

3.6. Test4 and Test5: central density

Figures 21 and 22 indicate that the central density has no influence on both the delivered power and the electric fields in front of the launcher. As a matter of fact, the fast wave is almost totally absorbed along the plasma column (single pass absorption considered in this tests is a reasonable assumption); therefore, the antenna behavior is mainly affected by the values assumed by the plasma profile (not varied in this case) around the cut-off of the dominant mode.

However, the reader can notice from figures 9 and 23 that, when also a part of the plasma edge is modified in order to change the central density, the aforementioned conclusions no longer hold true. To be more precise, the best performances in terms of delivered power and low RF potentials (namely Test5a case) are obtained with the lowest difference between the density values of the two sides of the outer gradient region (see figure 4 for the definition of the involved plasma regions); in other words, the smaller the density gap, the better the antenna behavior (figure 24).

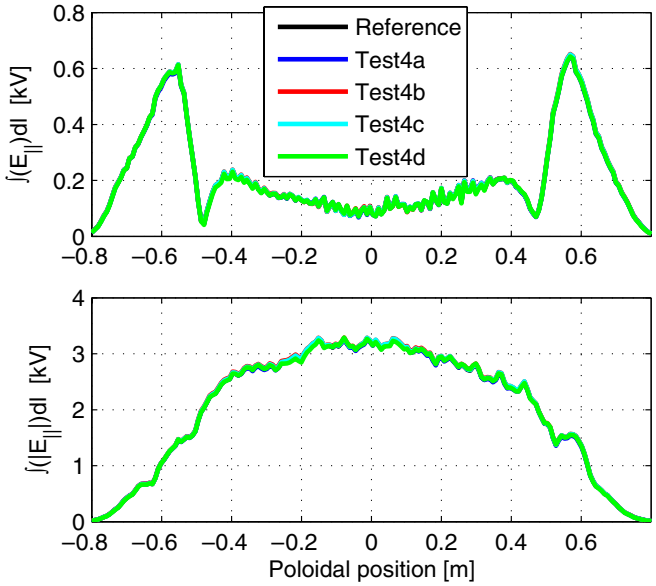

Figure 22. RF potentials (in kV) versus central density, computed integrating the parallel electric field (top, in magnitude) and its absolute value (bottom) along the magnetic field lines.

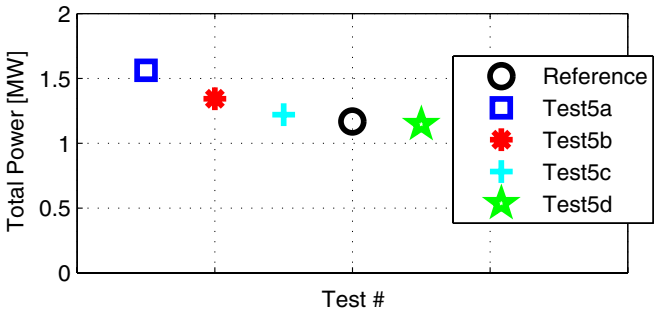

Figure 23. Power transferred to plasma (in MW) versus central density, assuming infinite coaxial lines connected to the ports, with a maximum voltage of 30 kV along the lines.

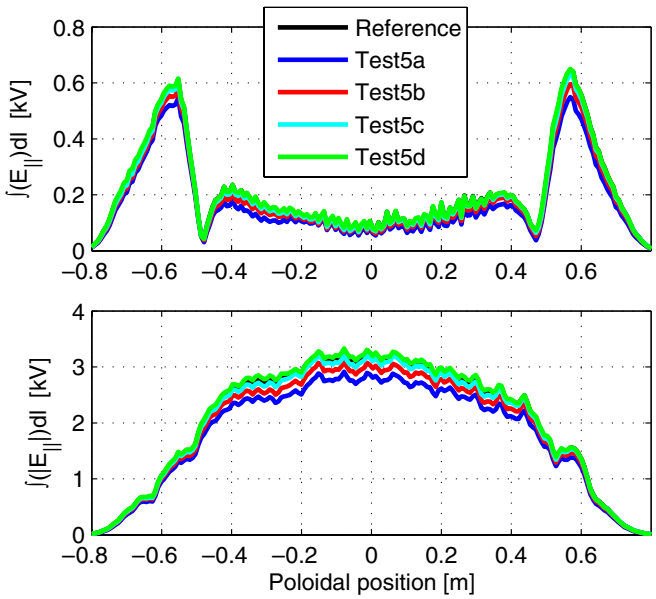

Figure 24. RF potentials (in kV) versus central density, computed integrating the parallel electric field (top, in magnitude) and its absolute value (bottom) along the magnetic field lines.

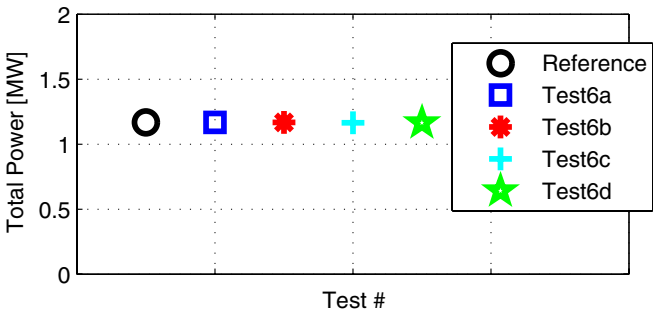

Figure 25. Power transferred to plasma (in MW) versus plasma temperature, assuming infinite coaxial lines connected to the ports, with a maximum voltage of 30 kV along the lines.

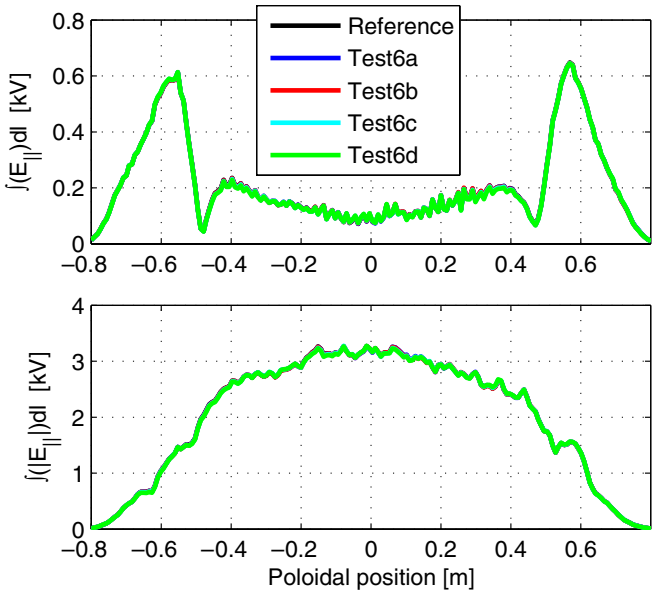

Figure 26. RF potentials (in kV) versus plasma temperature, computed integrating the parallel electric field (top, in magnitude) and its absolute value (bottom) along the magnetic field lines.

3.7. Test6: ion and electron temperature profile

Both the power transferred to plasma and the RF potentials are not influenced at all by an increase in the ion and electron temperature, as depicted in figures 25 and 26. Since, even with a global shift in the profile, the curves were practically overlapped, we decided not to further investigate the impact of the temperature with partial changes of the profile (i.e. varying only one portion of it), as performed with the electron density.

4. Conclusion and perspectives

The analysis of the main plasma density parameters performed in this paper showed that the power coupled to plasma is remarkably influenced by variations in the density gradient or in the edge density, while both the central electron density and the electron temperature are not relevant at all. Conversely, in terms of RF potentials, only the edge density, and in particular the equivalent vacuum inserted to approximate a (presumably not known) portion of the plasma profile, plays a fundamental role, considerably affecting the antenna performances. To summarize, the outlined tests demonstrated that not all plasma

parameters play the same role in determining the coupling properties of an IC antenna or its radiated electric field.

Once more, we are fully aware that these conclusions are intrinsically linked and limited to the simulated plasma profiles; however, even with the included 1D plasma model, the reliable knowledge of the plasma profile appears to be a crucial goal to be pursed. As a general conclusion, this paper stresses the importance of having accurate electron density measurement instruments available for the next generation of IC antennas, in order to allow numerical tools such as TOPICA to be as precise as possible during the analysis and design of IC launchers.

Acknowledgments

This work was carried out within the framework of the European Fusion Development Agreement no WP11-HCD-01-02-01-01. The views and opinions expressed herein do not necessarily reflect those of the European Commission. The authors gratefully acknowledge the valuable support of Dr R Bilato and Dr M Brambilla during the development and the testing of the code. Special thanks goes to Dr V Bobkov and Professor J-M Noterdaeme for the fruitful discussions about plasma profiles.

References

[1] Lancellotti V, Milanesio D, Maggiora R, Vecchi G and Kyrytsya V 2006 TOPICA: an accurate and efficient numerical tool for analysis and design of ICRH antennas *Nucl. Fusion* **46** S476–99

[2] Milanesio D, Meneghini O, Lancellotti V, Maggiora R and Vecchi G 2009 A multi-cavity approach for enhanced efficiency in TOPICA RF antenna code *Nucl. Fusion* **49** 115019

[3] Milanesio D, Maggiora R 2010 ITER ICRF antenna analysis and optimization using the TOPICA code *Nucl. Fusion* **50** 025007

[4] Durodié F *et al* 2012 Physics and engineering results obtained with the ion cyclotron range of frequencies ITER-like antenna on JET *Plasma Phys. Control. Fusion* **54** 074012

[5] Louche F, Dumortier P, Durodié F, Messiaen A, Maggiora R and Milanesio D 2011 3D modeling and optimization of the ITER ICRH antenna *19th Topical Conf. on Radio Frequency Power in Plasmas (Newport, RI)*

[6] Milanesio D, Ceccuzzi S, Maggiora R, Bobkov V and the ASDEX Upgrade Team 2011 Analysis of the impact of antenna and plasma models on RF potentials evaluation *19th Topical Conf. on Radio Frequency Power in Plasmas (Newport, RI)*

[7] Messiaen A, Koch R and Weynants R 2011 Influence of the edge plasma profile on the coupling of a ICRH antenna. Application to ITER *19th Topical Conf. on Radio Frequency Power in Plasmas (Newport, RI)*

[8] Maggiora R and Milanesio D 2011 Mitigation of parallel RF potentials by an appropriate antenna design using TOPICA *19th Topical Conf. on Radio Frequency Power in Plasmas (Newport, RI)*

[9] Brambilla M 1993 Modelling loop antennas for HF plasma heating in the ion cyclotron frequency range *Plasma Phys. Control. Fusion* **35** 41–62

[10] Brambilla M 1999 Numerical simulation of ion cyclotron waves in tokamak plasmas *Plasma Phys. Control. Fusion* **41** 1–34